

VIBRATION ANALYSIS OF CURVED FRAMES

Syam B K, Abhijit Sarkar, Priyadarshan P

Department of Mechanical Engineering, Indian Institute of Technology Madras Chennai, India
email:asarkar@iitm.ac.in

In many structural applications like bridges, arches, turbo-machineries blades, etc. curved frame structures are used and it is important to study its dynamic behavior. The use of a curvilinear coordinate system to solve such problems generates higher-order, complicated differential equations. Finite Element Method can be used to determine the dynamics of such structures. However, the high frequency simulation using FEM is inefficient and thus restricted in its applicability. The wave-based methods are advantageous in this regard. The wave methods have been well-developed for dealing with frame structures comprising of straight Euler-Bernoulli members with joints at an arbitrary angle. In such structures, the presence of the joint induces a coupling between the longitudinal and transverse dynamics. In the present work, we extend the wave-based technique to analyze frame structures comprising of filleted or circularly curved joints. The propagation matrix in the straight portion of the structure is well documented in the literature. In the present work, the curved portion of the structures is discretized into small linear segments, wherein each segment subtends a small angle with the neighboring segment. Using the continuity relations and equilibrium conditions at the joints, the reflection and transmission matrices at the joints can be obtained. The assembly of reflection, transmission and propagation matrices and the incorporation of the boundary conditions is in line with the standard wave method. Modal Analysis and Harmonic Analysis are conducted using the present approach and the results were found to correlate with those reported in literature as also with FEM simulations. The characterization of circular fillets in terms of its transmission and reflection effects is presented. The present method is computationally efficient for high frequency calculation in comparison to FEM simulation.

1. Introduction

In many structural applications like bridges, arches, pipings, scaffolding, etc. curved frames are used. Study of dynamic behaviour of such curved frame structures is important. Free vibration analysis of a planar circular curved frames was presented by Kang et. al. (2003)[1]. In their study, the curved frame included multiple point discontinuities such as elastic supports, attached masses, and curvature changes. Additionally, the authors also studied the dispersion equations and cut-off frequencies. Mei (2012)[5] performed free and forced vibration analysis of L-shaped frame and portal planar frame using wave propagation theory. Reflection and transmission matrices for the L joint were derived by Mei, considering the coupling effect of flexural and longitudinal motions. Mei (2008)[3] derived the transmission and reflection matrices for T-shaped and H-Shaped planar frame with different boundary conditions : (i) simply supported, (ii) clamped and (iii) free boundaries. Also, dynamic analysis of curved frame structures can be routinely performed using Finite Element Method (FEM). However, it is well-known that the FEM simulation is computationally intensive for high frequency range.

In Mei's work [5], wave propagation approach is applied to study an L-shaped frame with 90° corner joint. In this work, we extend the analysis reported in [5] by incorporating a circular-filleted

Nomenclature			
List of symbols			
a, b, c	amplitudes of waves	u	longitudinal displacement
$\{a\}, \{b\}, \{B\}$ etc	amplitudes of wave in vector format	V	shear force
A	area of cross-section	y	transverse displacement
E	Young's Modulus	ρ	density
h	thickness of the frame section	θ	angle subtended
F	normal force	ψ	rotary deflection
f	longitudinal force per length	ω	angular frequency
I	moment of inertia	subscripts	
i	complex unit	1, 2	frame 1 and frame 2
K	wavenumber	b	bending wave
L	length	c, f	clamped and free boundary
M	bending moment	h	horizontal
m	mass per unit length	j	joint
P	propagation matrix	v	vertical
p	transverse force per length	l	longitudinal wave
R	radius of curvature	n	near-field wave
R_{11}, R_{22}	reflection matrices	superscript	
t	time	+	positive going wave
T_{12}, T_{21}	transmission matrices	-	negative going wave

90° joint for a similar L-shaped frame structure (as shown in Figure 2a). The objective of this work is to evaluate the effect of fillet on the dynamic characteristics of the curved frame structure. The free and forced vibration characteristics of the curved frame structure is found using the wave-propagation based formulation. The results obtained are compared with ANSYS simulation results. The wave based method is computationally efficient and accurate in comparison to FEM simulations.

2. Methodology

For a frame structure, the axial motion and the transverse flexural motions are coupled. The governing equation for a transverse vibration using Euler-Bernoulli beam theory is given by

$$EI \frac{\partial^4 y}{\partial x^4} + m \frac{\partial^2 y}{\partial t^2} = p(x, t) \quad (1)$$

The governing equation for the longitudinal vibration is formulated as

$$EA \frac{\partial^2 u}{\partial x^2} - m \frac{\partial^2 u}{\partial t^2} = -f(x, t) \quad (2)$$

In both these equations x denotes the axial direction of the one-dimensional structure. p is transverse load per unit length in the transverse direction, f is the axial load per unit length.

In the absence of external forcing (p and f) and by assuming harmonic time dependency ($e^{i\omega t}$) the solution of the homogeneous part of equations(1) and (2) can be written as

$$y(x) = a_1^+ e^{-ik_b x} + a_2^+ e^{-k_n x} + a_1^- e^{ik_b x} + a_2^- e^{k_n x} \quad (3)$$

$$u(x) = a_3^+ e^{-ik_l x} + a_3^- e^{ik_l x} \quad (4)$$

where a_i 's are the complex amplitudes. The wavenumbers are given by

$$k_b = k_n = \sqrt[4]{\frac{m\omega^2}{EI}}; \quad k_l = \sqrt{\frac{m}{EA}}\omega \quad (5)$$

2.1 Propagation

Consider a straight segment of the frame as shown in figure(1c). Let B and C be two points separated by an arbitrary distance x as shown in the figure. The amplitude of the forward waves at B can be related to the amplitude of the forward waves at C using the propagation matrix P which in turn depends on the wavenumbers and the distance between the points B and C [1].

$$\{B^+\} = [P(x)]\{C^+\}, \{B^-\} = [P(x)]^{-1}\{C^-\} \quad (6)$$

where, $\{B\}, \{C\}$ are column vectors having three elements. It contains propagating bending wave component, evanescent wave component and traveling longitudinal wave coefficient, respectively. Here, the propagation matrix is given by [3]

$$[P(x)] = \begin{bmatrix} e^{-ik_1x} & 0 & 0 \\ 0 & e^{-k_2x} & 0 \\ 0 & 0 & e^{-ik_3x} \end{bmatrix} \quad (7)$$

2.2 Reflection and Transmission for an Angular joint

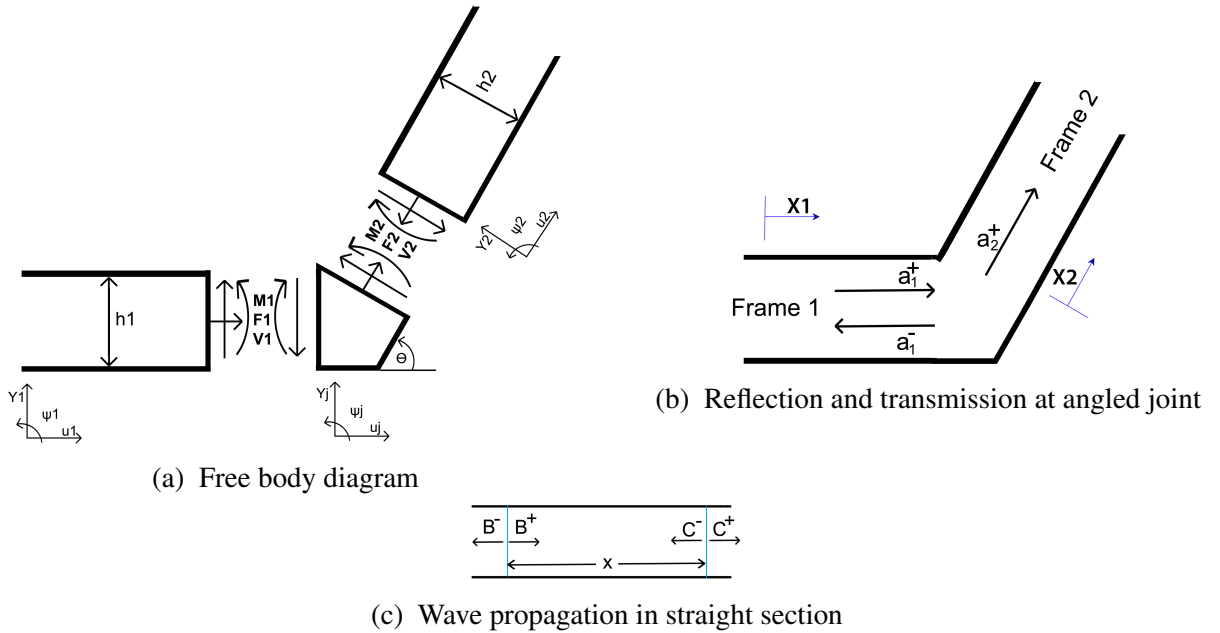


Figure 1

Similar to propagation matrix discussed above, the reflection and transmission matrices relate the incident wave amplitudes to the reflected and transmitted wave amplitudes. The reflection and transmission matrices associated with 90° corner joints have been derived by Mei [3]. In the following, we derive the reflection and transmission matrices associated with an arbitrary angular corner joint.

Let us assume a semi-infinite frame structure whose leg 2 is infinite. The reflection and transmission matrix corresponding to an incident amplitude vector $\{a_1^+\}$ is given as

$$\{a_1^-\} = [R_{11}]\{a_1^+\}, \{a_2^+\} = [T_{12}]\{a_1^+\} \quad (8)$$



Figure 2

The transverse and longitudinal deflection of frame 1 at any point can be expressed as

$$y_1(x_1) = a_{1b}^+ e^{-ik_b x_1} + a_{1n}^+ e^{-k_n x_1} + a_{1b}^- e^{ik_b x_1} + a_{1n}^- e^{k_n x_1} \quad (9a)$$

$$u_1(x_1) = a_1^+ e^{-ik_l x_1} + a_1^- e^{ik_l x_1} \quad (9b)$$

Frame 2 has only forward moving wave as it is infinite and its transverse and longitudinal deflection can be represented in terms of x as

$$y_2(x_2) = a_{2b}^+ e^{-ik_b x_2} + a_{2n}^+ e^{-k_n x_2} \quad (10a)$$

$$u_2(x_2) = a_{2l}^+ e^{-ik_l x_2} \quad (10b)$$

The forces and moments generated in frame1 and frame 2 can be related in terms of deflection as shown below,

$$M_1 = EI \frac{\partial^2 y_1}{\partial x_1^2}, V_1 = -EI \frac{\partial^3 y_1}{\partial x_1^3}, F_1 = EA \frac{\partial u_1}{\partial x_1} \quad (11a)$$

$$M_2 = EI \frac{\partial^2 y_{21}}{\partial x_2^2}, V_2 = -EI \frac{\partial^3 y_2}{\partial x_2^3}, F_2 = EA \frac{\partial u_2}{\partial x_2} \quad (11b)$$

Invoking equilibrium conditions and kinematic continuity at the angular joint (free body diagram of the angular joint is shown in Figure 1a), we obtain six equations relating the wave amplitudes. These are represented in a compact matrix notation as follows

$$[N1]a_2^+ - [N2]a_1^- = [N3]a_1^+ \quad (12a)$$

$$[N4]a_2^+ - [N5]a_1^- = [N6]a_1^+ \quad (12b)$$

Rearranging and simplifying these equations, yield the transmission and reflection matrix of the angular joint as

$$[T_{12}] = \left[[N2]^{-1}[N1] - [N5]^{-1}[N4] \right]^{-1} \left[[N2]^{-1}[N3] - [N5]^{-1}[N6] \right] \quad (13a)$$

$$[R_{11}] = \left[[N4]^{-1}[N5] - [N1]^{-1}[N2] \right]^{-1} \left[[N1]^{-1}[N3] - [N4]^{-1}[N6] \right] \quad (13b)$$

A similar procedure is carried out to obtain the transmission and reflection matrices due to an incident wave vector in Frame 2. These matrices are defined as T_{21} and R_{22} , respectively.

2.3 Boundary Condition

The reflection matrices at clamped and free boundaries are derived by Mace [2]. These matrices given by R_c and R_f are given as

$$[R_c] = \begin{bmatrix} -i & -1-i & 0 \\ -1+i & i & 0 \\ 0 & 0 & -1 \end{bmatrix}, [R_f] = \begin{bmatrix} -i & -1+i & 0 \\ 1-1 & i & 0 \\ 0 & 0 & 1 \end{bmatrix} \quad (14)$$

2.4 Discretization & Assembly

In the following, a brief description of the interrelationship of the wave amplitudes at the different sections of the structure is presented. The curved section of the structure is discretized into N small linear segments as shown in figure(2a). Note, the successive segments subtends an angle with the other. This generates a discontinuity at the junction of two segments due to change in direction as shown in the figure(2a).

The relation between wave amplitudes at the boundaries is given by

$$[I]\{a^+\} = [R_c]\{a^-\}, \quad [I]\{b^-\} = [R_f]\{b^+\}. \quad (15)$$

Here, $[I]$ is the 3×3 identity matrix. Along the straight horizontal section, the wave components at points A and C are related by propagation matrix

$$[I]\{c_1^+\} = [P(L_h)]\{a^+\}, \quad [I]\{c_1^-\} = [P(L_h)]^{-1}\{a^-\} \quad (16)$$

, where L_h is the length of the horizontal section. The curved section between C and E is discretized into number of linear elements of equal size as shown in figure(2a). Two sets of reflection and transmission matrices derived earlier are used to find the relation between wave amplitudes at point C and are given by

$$[T_{12}]\{c_1^+\} + [R_{22}]\{c_2^-\} = [I]\{c_2^+\}, \quad [T_{21}]\{c_2^-\} + [R_{11}]\{c_1^+\} = [I]\{c_1^-\} \quad (17)$$

Similarly, the wave amplitude relation at point D in figure(2a) can expressed in terms of reflection and transmission matrices as follows

$$[T_{12}]\{d_1^+\} + [R_{22}]\{d_2^-\} = [I]\{d_2^+\}, \quad [T_{21}]\{d_2^-\} + [R_{11}]\{d_1^+\} = [I]\{d_1^-\} \quad (18)$$

However, points C and D can also be related by propagation matrix since it forms a straight element.

$$[I]\{d_1^+\} = [P(l)]\{c_2^+\}, \quad [I]\{d_1^-\} = [P(l)]^{-1}\{c_2^-\} \quad (19)$$

Similarly, the wave amplitude relationships for all consecutive interim points in between D and E are arrived at. Finally, wave amplitudes at B and E are also related by the propagation matrix

$$[I]\{b^+\} = [P(L_v)]\{e_2^+\}, \quad [I]\{b^-\} = [P(L_v)]^{-1}\{e_2^-\} \quad (20)$$

where, L_v represents the length of the vertical section

Assembly of the above equations leads to a matrix equation of the form $[A(\omega)]\{X\} = \{0\}$. Here, $[A]$ is a square matrix of size $12 \times (N + 1)$. $\{X\}$ is column vector having $12 \times (N + 1)$ elements representing wave amplitudes. For non-trivial solution, the roots of the characteristic equation is solved numerically. These roots denote the natural frequencies of the system.

The wave propagation based method can also be extended for the forced vibration analysis. Towards this end, we note that application of a point loading induces different waves on either side of the

point of application of the load. As an illustration, in figure(2a) a point harmonic forcing is applied at the point G. In the portion to the left of G, there is a forward wave of amplitude $\{g_{11}^+\}$ and a backward wave of amplitude $\{g_{11}^-\}$. Analogously, in the portion to the right of G, there is a forward wave of amplitude $\{g_{12}^+\}$ and a backward wave of amplitude $\{g_{12}^-\}$. These wave amplitudes are related by the following equation (as derived by Mei [4])

$$[I]\{g_{12}^+\} - [I]\{g_{11}^+\} = [I]\{f\}, \quad [I]\{g_{12}^-\} - [I]\{g_{11}^-\} = [I]\{-f\} \quad (21)$$

$$\text{where } \{f\} = \frac{F}{4EIK_b^3} \begin{Bmatrix} -i \\ -1 \\ 0 \end{Bmatrix}$$

Here, F represents the magnitude of the harmonic transverse force applied on the frame structure. Due to this force the propagation matrix will also get modified as follows

$$\begin{aligned} [I]\{g_{11}^+\} &= [P(L_{h1})]\{a^+\}, & [I]\{g_{11}^-\} &= [P(L_{h1})]^{-1}\{a^-\}, \\ [I]\{c_1^+\} &= [P(L_{h2})]\{g_{12}^+\}, & [I]\{c_1^-\} &= [P(L_{h2})]^{-1}\{g_{12}^-\} \end{aligned} \quad (22)$$

In contrast to free vibration analysis, for forced vibration analysis equation(22) is used instead of equation(16). All other equations arrived at for the free vibration analysis carry over to the forced vibration analysis also. By incorporating these equations, a system of matrix equation of the form, $[A_f(w)]\{X_f\} = \{F\}$ is obtained. For forced vibration analysis A is a square matrix of size $12 \times (N + 2)$. Similarly, $\{X_f\}$ and $\{F\}$ are column vectors having $12 \times (N + 2)$ elements representing the wave amplitude and force, respectively.

2.5 Free vibration analysis

For the present work, one end of the frame is free and the other end is fixed. The physical properties of the frame used are Young's modulus $E = 2 \times 10^9 N/m^2$, Mass Density $M = 7800 Kg/m^3$, Poisson's ratio $\nu = 0.30$, the cross-sectional width and breadth being $0.0127m$ each. The length of each arm is $0.5m$, with radius of curvature $R = 0.5m$ and angle of 90° degrees. For the present problem, the curved structure is divided into 30 elements. Reflection and transmission of waves occur at each junction of these elements. Along with propagation matrix, boundary conditions, reflection matrix and transmission matrix at each discontinuity, a global matrix of size 372×372 is derived. Natural frequencies are obtained by finding the eigen value of this matrix. The corresponding eigen vectors are the mode shapes. The results obtained using the present method are compared with results obtained using Finite Element Method commercial package (Ansys). These results are presented in figure(3). The modal analysis shows good correlation between the present wave based method and the results obtained using ANSYS.

As discussed earlier, an objective of the current investigation is to determine the effect of the fillet radius on the dynamics of the structure. Towards this end, keeping all the parameters of the frame constant eg: mass, area of cross-section etc, variation of the natural frequency with respect to change in radius of curvature was obtained. The frame structure discussed above is analyzed with varying radius of the interconnecting fillet. The fillet radius is varied keeping the mass of the structure fixed. Accordingly, the length of the horizontal and vertical arms of the structure change with changing fillet radius. Finally, the natural frequencies obtained are non-dimensionalized with respect to the natural frequencies for a L-shaped structure (*viz.* zero fillet radius). The results for the variation of the natural frequencies of the first three modes with increasing fillet radius are shown in Figure 5. The results obtained using ANSYS are also presented alongside for comparison.

Forom, these results it is found out that the fundamental natural frequency shows a decreasing characteristics whereas the second natural frequency is exhibiting an increasing trend. It is interesting to note that third mode is exhibiting a stiffening characteristics beyond a critical value of fillet radius.

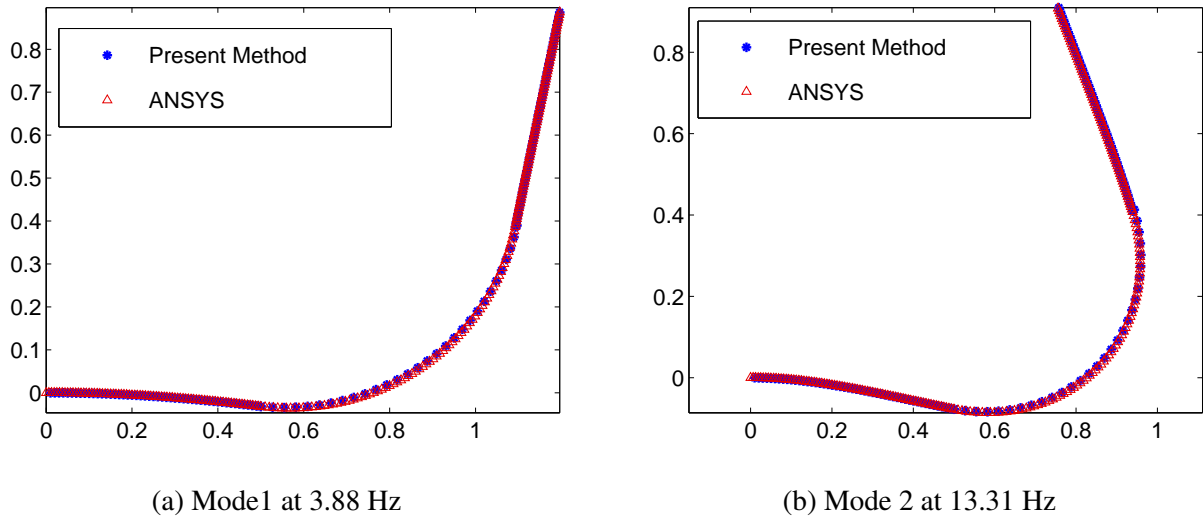


Figure 3: Comparison of modal analysis results obtained using the present method and ANSYS.

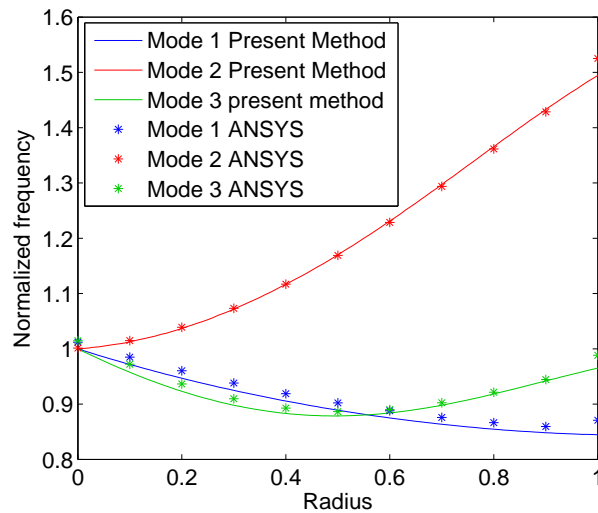


Figure 4: Change of normalized natural frequency with respect to radius

2.6 Forced Vibration Analysis

A harmonic forcing of unit amplitude is imparted at the midpoint of the horizontal section. Under this condition, the response at the tip of vertical section is calculated as shown in figure(2b). Due to the forcing function additional discontinuity will be created at the point where the load is applied. As a consequence, the propagation matrix has been modified. The curved portion of the frame is discretized into 30 linear elements. So the system of equations can be written as $AX = F$ where A is the global matrix whose size has been increased to 384×384 . X and F corresponds to column vectors of, 384×1 representing the wave amplitude, and applied force, respectively. The transverse deflection of any point in the frame is obtained by adding the transverse component(propagating and evanescent)of the wave amplitude(forward and backward) at that point. Identical procedure is carried on the longitudinal component of the wave amplitude so as to obtain the longitudinal deflection. Both the frequency response function(fig(5a)) and the operational deflection shape(fig(5b)) obtained through this approach shows good match with the corresponding ANSYS results. For the purpose of visualization, the operational deflection shape is scaled by 10^5 times. Here again, we observe a good correlation of the results obtained by the two methods.

In the frequency response function(5a), it is observed that at low frequencies the response ob-

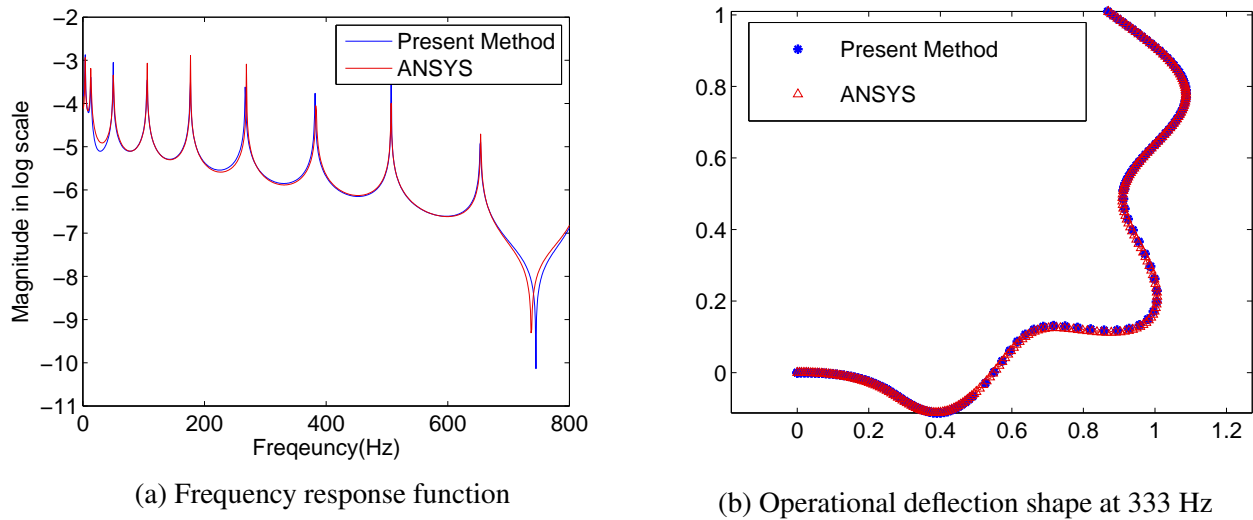


Figure 5

tained through present method shows some mismatch with FEM. At these frequencies the wavelength is comparable to the arc length of the curved structure. Extensional mode dominates at these frequencies. This can be captured using curvilinear co-ordinate system and is well described in ref([1]).

3. Conclusion

In this paper, wave method is employed to analyze the in-plane vibration of a curved frame structure. The coupling effect between the longitudinal and transverse vibrations is considered. Reflection and transmission matrices for the angled joint are derived. The result shows good agreement with FEM results. High frequency dynamical simulation through FEM is known to be computationally intensive. A finer mesh at high frequencies leads to larger matrix size for the FEM simulation. In this respect, the proposed wave-based method is more efficient. This method yields the same matrix size irrespective of the frequency. Also, the accuracy is not compromised at the higher frequencies. The present work assumed Euler-Bernoulli beam theory. However, at high frequencies the effects of rotary inertia and shear distortion comes into picture. This can be tackled by utilizing Timoshenko beam theory instead of Euler-Bernoulli beam theory.

References

1. B Kang, C H Riedel, and C A Tan. Free vibration analysis of planar curved beams by wave propagation. *Journal of Sound and Vibration*, 260(1):19–44, 2003.
2. B R Mace. Wave reflection and transmission in beams. *Journal of Sound and Vibration*, 97(2):237–246, 1984.
3. C Mei. Wave analysis of in-plane vibrations of h-and t-shaped planar frame structures. *Journal of Vibration and Acoustics*, 130(6):061004, 2008.
4. C Mei. In-plane vibrations of classical planar frame structures an exact wave-based analytical solution. *Journal of Vibration and Control*, 16(9):1265–1285, 2010.
5. C Mei. Wave analysis of in-plane vibrations of l-shaped and portal planar frame structures. *Journal of Vibration and Acoustics*, 134(2):021011, 2012.